Implication of Climate Change On Crop Water Requirement: A Regional Case Study in The Semi-Arid Region of Western Maharashtra, India

Shubham Anil Gade (shubhamgade66@gmail.com)
Mahatma Phule Krishi Vidyapeeth https://orcid.org/0000-0003-1671-8394
Devidas D Khedkar
Interfaculty Department of Irrigation and Water Management

Research Article

Keywords: Statistical DownScaling Model, Climate change, HadCM3, Western Maharashtra, Reference crop evapotranspiration, Crop water requirement

Posted Date: October 28th, 2021

DOI: https://doi.org/10.21203/rs.3.rs-931698/v1

Implication of Climate Change on Crop Water Requirement: A Regional Case Study in the semi-arid region of Western Maharashtra, India

Shubham A Gade [a,*] and Devidas D Khedkar [b]

[a] *Young Professional-II, School of Atmospheric Stress Management, National Institute of Abiotic Stress Management, ICAR, Baramati, 413 115 (M.S.), India. Email: shubhamgade66@gmail.com*

[b] *Assistant Professor, Interfaculty Department of Irrigation and Water Management, MPKV, Rahuri 413 722 (M.S.), India. Email- devidaskhedkar@gmail.com*

Implication of Climate Change on Crop Water Requirement: A Regional Case Study in the semi-arid region of Western Maharashtra, India

Abstract

The hydrological cycle has been massively impacted by climate change and human activities. Thus it is of the highest concern to examine the effect of climate change on water management, especially at the regional level, to understand possible future shifts in water supply and water-related crises, and to provide support for regional water management. Fortunately, there arises a high degree of ambiguity in determining the effect of climate change on water requirements. In this paper, the Statistical DownScaling (SDSM) model is applied to simulate the potential impact of climate on crop water requirement (CWR) by downscaling ET_0 in the region of Western Maharashtra, India for the future periods *viz.,* 2030s, 2050s, and 2080s across three meteorological stations (Pune, Rahuri, and Solapur). Four crops i.e. cotton, soybean, onion, and sugarcane are selected during the analysis. The Penman-Monteith equation is used to calculate reference crop evapotranspiration (ET_0), which further in conjunction with the crop coefficient (K_c) equation is used to calculate crop evapotranspiration (ET_c) / CWR. The predictor variables are extracted from the NCEP reanalysis dataset for the period 1961-2000 and the HadCM3 under H3A2 and H3B2 scenarios for the period of 1961 – 2099. The results indicated by SDSM profound good applicability in downscaling due to satisfactory performance during calibration and validation for all three stations. The projected ET_0 indicated an increase in mean annual ET_0 as compared to the present condition during the 2030s, 2050s, and 2080s. The ET_0 would increase for all months (in summer, winter, and pre-monsoon seasons) and decrease from June to September (monsoon season). The estimated future CWR show variation in the range for cotton (-0.97 to 2.48%), soybean (-2.09 to 1.63 %), onion (0.49 to 4.62 %), and sugarcane (0.05 to 2.86 %).

Keywords: Statistical DownScaling Model, Climate change, HadCM3, Western Maharashtra, Reference crop evapotranspiration, Crop water requirement

1. Introduction

Climate change is becoming trouble and the hottest topic on the entire globe. Extreme warming caused by human emission of greenhouse gases and the subsequent large-scale changes in weather patterns confronts climate change. Most Asian countries have witnessed more frequent floods and droughts over the last decades due to climate change and human activities (Zhai et al. 2005; Kranz et al. 2010; Xu et al. 2013). According to the 5th Assessment Report of the Intergovernmental Panel on Climate Change (IPCC), the global warming trend will continue, result mainly caused by the increasing amount of greenhouse gas emissions (IPCC, 2013; Tao et al., 2015).

As per IPCC, during the years 1880-2012, the global surface temperature rose by 0.65-1.06 ºC, and the pace of increase after 1951 was around 0.12 ºC per 10 years, which is almost double the rate since 1880

(Zhou et al. 2017). The effects of global climate change on hydrological parameters such as runoff, evapotranspiration (ET_0), surface storage, and soil moisture are needed to be explored in order to determine water supply conditions (Xu et al. 2013; Rajabi and Babakhani 2018). Global agriculture has impacted climate change in recent decades and is one of the threats of increasing food demand for the rapidly growing population under intensified environmental stress. Worldwide, due to global warming, a shift in the atmosphere is anticipated and contributed to the fluctuations in CWR.

The knowledge of the water requirements of various crops is supposed to predict for balancing the water demand and the water fluctuations for effective management. Global agriculture impacted by climate change in recent decades is one of the main challenges of rising food supply for the rapidly growing population. The regional cropping calendar, cropping system, growing season, crop water requirement (CWR) and irrigation requirement (IR) for different agro-climatic zone relies on the respective climatic parameters such as precipitation, temperature, relative humidity, evapotranspiration, wind speed, sunshine hours, etc. (Goyal 2004; Thomas 2008). It was analyzed that seasonal rainfall (June-Sept) in Maharashtra had a direct impact on soil moisture variation (Gade et al. 2021). Furthermore, the agriculture sector and CWR are more sensitive and affected by climate variability through climate extreme events such as drought, flood, and heatwaves.

Past studies (IPCC 2002, 2007, 2013; Pandey et al. 2008) have revealed that worldwide meteorological parameters *viz.,* precipitation, temperature, evapotranspiration, wind speed, sunshine hours, etc. are fluctuating from the normal in last century. These are due to both natural as well as anthropogenic factors. Temperature is a prime climatic variable for the water allocation and farming sector after the precipitation (Duhan et al. 2013). Studies have also shown that temperature level is rising with latitudes in the Northern Hemisphere (Kumar 2007)**.** (Goyal 2004) conducted a sensitivity analysis of the evapotranspiration rate over Rajasthan, India. The results suggested that the evapotranspiration rate rises by 14.8%, with a significant increase in temperature by 20%.

Crop evapotranspiration (ETc) varies significantly from ET_0 as soil cover, canopy properties, and crop aerodynamic resistance. Due to alterations in crop characteristics during the growing season, the crop coefficients for the particular crop change from sowing to harvesting. As a result, different crops would have different crop coefficients. The crop coefficient also influences the varying properties of the crop during its growth. The Penman-Monteith (P-M) is still the only standard method under all climatic conditions recommended by FAO 56 (Allen et al. 1998). Potential climate change significantly affects agriculture and water supplies, in a nutshell, the crop production sector should be more conscious of productive approaches for the application and storage of water. (Doria et al. 2006) have demonstrated simulation reliant on both natural and anthropogenic radiative forcing this is more closely associated with observed data, which only accounts natural climatic conditions.

Many downscaling methodologies have been proposed in the last two decades, this recognizes the temporal and spatial mismatch between the regional scales and the gross scales. Initially, these techniques were mainly used in Europe and the United States (Wilby and Wigley 1997). Downscaling approaches have emerged as effective methods to reduce the problem of indistinct scales by deriving regional climate detail from global climate data (Gagnon et al. 2005). Various researchers (Wang et al. 2013; Xu et al. 2014; Tao et al. 2015; Manasa and Shivapur 2016; Kundu et al. 2017; Zhou et al. 2017; Guo et al. 2018) downscaled ET_0 using SDSM and other models and found significant variations in contrast to current conditions. The statistical downscaling is based on few assumptions, these are the predictor – predictand relationships are valid under future climatic conditions and predictor variables with their changes well-characterized by GCMs (Wilby and Wigley 2000; Saraf and Regulwar 2016). Studies in the Tibetan plateau by (Wang et al. 2013) projected ET_0 during 2011–2100 from the HadCM3 and CGCM3 model, where SDSM performed satisfactorily in downscaling ET_0, and the continuous increment in ET_0 observed in the 21st century. (Guo et al. 2018) analyzed the evaluation indices (R^2, *Ens*) during calibration and validation periods, the results indicated fair simulation of temperature and evapotranspiration by SDSM model. The SDSM is the combination of multiple regression and a stochastic weather generator (Gebremeskel et al. 2004; Mahmood and Babel 2013).

Although climate projection of rainfall and temperature are frequent, there's been limited research on the generation of future ET_0 (Kundu et al. 2017). However, ET_0 is not only a crucial climatic parameter controlling the water balance but also a key factor influencing crop production. In the semi-arid areas of less rainfall or rainfall-based agricultural season (as Western Maharashtra), variation in crop water requirement may create a problem. In the region, the future projection of ET_0 has not been done before. Therefore, it is necessary to study variations in ET_0 and evaluate their effectiveness in the future and develop better management strategies.

2. Materials and Methods

2.1. Study area description

The investigation was carried out for the region in Western Maharashtra, agro-climatic region of Maharashtra in the western province of India to analyze the variability of crop water requirement of primary crops grown in the region. The major crops grown in the study area are cotton, onion, soybean, sugarcane, groundnut, sorghum, and maize. The average annual rainfall in the region ranges from 608-635 mm. The climate of Western Maharashtra is hot and dry. The 89% of annual rainfall in the central part during southwest monsoon rainfall is received during June to September, with 37 rainy days out of 122 days having daily rainfall (r >= 2.5) (Guhathakurta et al. 2020).The average annual rainfall decreases from 852 mm on the southern side to 567.5 mm on the northern side (TERI 2014). Western Maharashtra is more irrigated than the rest of Maharashtra. The geology of the region is dominated by basaltic rock. The study area occupied the largest

share (50 percent) in the gross irrigated area of the state since most of the rivers originate from Western Ghats mountain ranges and are diverted to the east through Western Maharashtra. The irrigation potential of 4.826 × 106 ha-m has been created by the Water Resources Department of the state through 3,712 completed and ongoing projects (Audit 2018). The conditions adversely affect the socio-economic conditions of the people, who are mainly dependent on agriculture. It also has a phenomenal impact on crop water requirements.

2.2. Location of study area

The area for the study is in the Western Maharashtra region bounded by latitude 17º 39' to 19º 24' N to 73º 50' to 75º 55' E. The selected stations over the region with name, latitude, longitude, and altitude are represented in

Table 1. The boundary map of the study area with selected stations is depicted in **Fig. 1**.

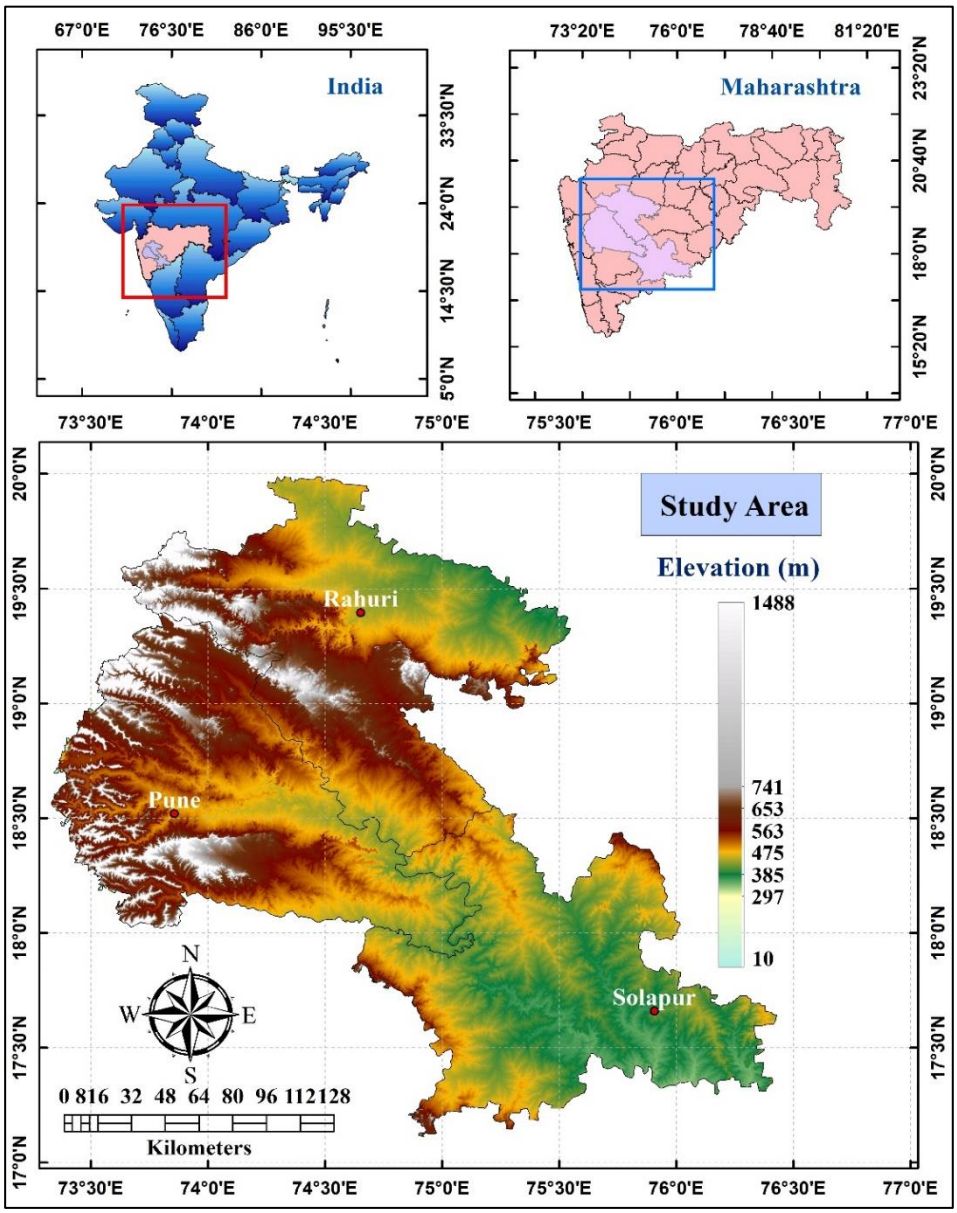

Fig. 1. The location map of Western Maharashtra.

Table 1 The details of the meteorological stations under the study area

Sr. No	District	Station	Latitude	Longitude	Altitude	Data
1.	Ahmednagar	Rahuri	19^0 23' 33"N	74^0 38' 56"E	514.55 m	1975 - 2000
2.	Pune	Pune	18^0 31' 13"N	73^0 51' 24"E	559.90 m	1970 - 2000
3.	Solapur	Solapur	17^0 40' 08"N	75^0 54' 24"E	483.50 m	1967 - 2000

2.3. Data Acquisition

2.3.1. Geographical Data:

2.3.2. Meteorological Data:

The climatic parameters as maximum temperature, minimum temperature, maximum relative humidity,

minimum relative humidity, bright sunshine hour, and wind speed) were used for the estimation of reference crop evapotranspiration. The data was acquired from Indian Meteorological Department (IMD), Pune and SAU, Rahuri for selected stations. It was available as a continuous record of daily format.

2.3.3. Reanalysis Data:

The estimation of future crop water requirements was done by downscaling of observed ET0. It requires reanalysis of NCEP and GCM data along with observed meteorological data of the study area. The National Centre for Environmental Prediction (NCEP) provides daily reanalysis data of 26 factors, including mean temperature, mean sea level pressure, near surface relative humidity, near surface specific humidity, 500 hPa geopotential height, 850 hPa geopotential height and relative humidity, geostrophic airflow velocity, vorticity, zonal velocity component, meridional velocity component, wind direction and divergence at the surface, 500 hPa height, and 850 hPa height (Zhou et al. 2017). Table 5 describes the predictors along with descriptions. The grid resolution is 2.5 degrees of latitude by 2.5 degrees of longitude. This data is available on the Canadian Climate Impact Scenarios (CCIS) website (Guo et al. 2018).

2.3.4. GCM Data:

The General circulation model (GCM) data was used for generating different scenarios generation. The GCM selected was Hadley Centre Coupled Model version 3 (HadCM3). HadCM3 is a coupled climate model with a horizontal resolution of 2.5 degrees of latitude by 3.75 degrees of longitude, and the predictors were the same as NCEP data. The predictor variables are available for the period 1961-2099 (Saraf and Regulwar 2016). Furthermore, this model has been extensively used in the statistical downscaling of climatic variables across the Indian sub-continent (Anandhi et al. 2008; Mahmood and Babel 2013; Saraf and Regulwar 2016). The output of the HadCM3 consists of two scenarios (H3A2 and H3B2), both scenarios utilized in the study.

2.4. Estimation of Crop Water Requirement (CWR)

The estimation of CWR is one of the basic needs for crop planning of any irrigation project. The water requirement is specified as the quantity of water, regardless of its source, needed by a crop or diversified crop pattern for its growth under field conditions in a given period (Micheal 2008). The water requirement encompasses losses due to crop evapotranspiration (ETc) or consumptive use (Cu). In addition to losses during water use (inevitable losses), seepage losses.

$$WR = ET_c \text{ or } C_u + \text{application losses} \quad \ldots. (1)$$

The water requirement for plants is, therefore, a 'demand' and 'supply' consisting of a contribution from any source of water, the primary source being irrigation water (IR), effective rainfall (ER), and soil profile contribution (S). Here, water requirement was estimated considering the demand side and nullifying the

losses due to application as these parameters vary from place to place. The crop evapotranspiration is calculated by the following relationship,

$$ET_C = ET_0 \times K_C \quad \text{.... (2)}$$

Where, ET_c = Crop evapotranspiration (mm/day); ET_0 = Reference crop evapotranspiration (mm/day); and, K_c = Crop coefficient (dimensionless)

The (ET_0) was calculated using the FAO 56 Penman-Monteith method (Allen et al. 1998), it is recommended as the sole method for determining ET_0 and is represented as:

$$ET_0 = \frac{0.408 * \Delta * (R_n - G) + \gamma * \left(\frac{900}{T + 273}\right) * U_2 * (e_s - e_a)}{\Delta + \gamma * (1 + 0.34 * U_2)} \quad \text{.... (3)}$$

Where,

ET_0 = Reference crop evapotranspiration (mm/day); Δ = Slope of saturation vapour pressure temperature curve (kPa/^{0}C); γ = Psychometric constant (kPa/^{0}C); T=Mean air temperature (^{0}C); e_s= Saturated vapour pressure (kPa); e_a= Actual vapour pressure (kPa); R_n= Net radiation (MJ/m^2/day); G = Soil heat flux density (MJ/m^2/day); U_2 = Wind speed at 2m height (m/s) and; (e_s - e_a) = Saturated vapour pressure deficit (kPa)

The net radiation was estimated as follows:

$$R_n = 0.77\left(a + b\frac{n}{N}\right)R_a - R_{nl} \quad \text{.... (4)}$$

Where, a and b are empirical coefficients (a = 0.18 and b = 0.55); *n (h)* is the sunshine duration; *N* (h) is the maximum sunshine duration; R_a (MJ/m^2.d) is the extraterrestrial radiation; and R_{nl} (MJ/m^2.d) is the net outgoing longwave radiation (Zotarelli et al. 2010; Wang et al. 2019).

2.4.1. Details of Selected Crops

For estimation of crop water requirement cotton, onion, soybean, and sugarcane crops were selected as they are majorly grown in the study region. The details of selected crops for analysis with their growth period, duration, and season are described in Table 2.

Table 2 Details of selected crop with growth period

Crops	Sowing Date	Harvesting Date	Duration	Season
Cotton	15 May	10 Nov.	180 Days	*Kharif*
Onion	15 Oct.	11 Feb.	120 Days	*Rabi*
Soybean	1 July	8 Oct.	100 Days	*Kharif*
Sugarcane	30 Jan.	29 Jan.	365 Days	*Perennial*

2.4.2. Crop Coefficient (Kc) Equations

The crop coefficient varies with crop growth stages. The Kc values were interpolated for the initial stage,

development mid-season stage, and late-season stages. The daily Kc values for different crops for the Rahuri region during their entire growth were calculated by the polynomial equations generated by the Department of Irrigation and Drainage Engineering and recommended by Mahatma Phule Agriculture University, Rahuri (India). It was assumed that the equations are valid over the entire study area and do not change concerning place and time. The details of the Kc equation for cotton, onion, soybean and sugarcane are well-illustrated below in Table 3 and Fig. 2 where t= Day since sowing; T= Total crop growth period in days.

Table 3 The Kc equation for cotton, onion, soybean and sugarcane

Crops	**Polynomial equation**
Cotton	$K_{ct} = 18.78 * \left(\frac{t}{T}\right)^4 - 39.98 * \left(\frac{t}{T}\right)^3 + 24.06 * \left(\frac{t}{T}\right)^2 - 2.89 * \left(\frac{t}{T}\right) + 0.453$
Onion	$\mathrm{K_{ct}} = 8.062 * \left(\frac{\mathrm{t}}{\mathrm{T}}\right)^5 - 24.31 * \left(\frac{\mathrm{t}}{\mathrm{T}}\right)^4 + 20.15 * \left(\frac{\mathrm{t}}{\mathrm{T}}\right)^3 - 5.76 * \left(\frac{\mathrm{t}}{\mathrm{T}}\right)^2 + 1.498 * \left(\frac{\mathrm{t}}{\mathrm{T}}\right) + 0.561$
Soybean	$K_{ct} = 2.647 * \left(\frac{t}{T}\right)^5 + 0.14 * \left(\frac{t}{T}\right)^4 - 8.76 * \left(\frac{t}{T}\right)^3 + 5.862 * \left(\frac{t}{T}\right)^2 + 0.26 * \left(\frac{t}{T}\right) + 0.494$
Sugarcane	$\mathrm{K_{ct}} = 0.484 * \left(\frac{\mathrm{t}}{\mathrm{T}}\right)^4 - 4.948 * \left(\frac{\mathrm{t}}{\mathrm{T}}\right)^3 + 3.988 * \left(\frac{\mathrm{t}}{\mathrm{T}}\right)^2 + 0.636 * \left(\frac{\mathrm{t}}{\mathrm{T}}\right) + 1.498$

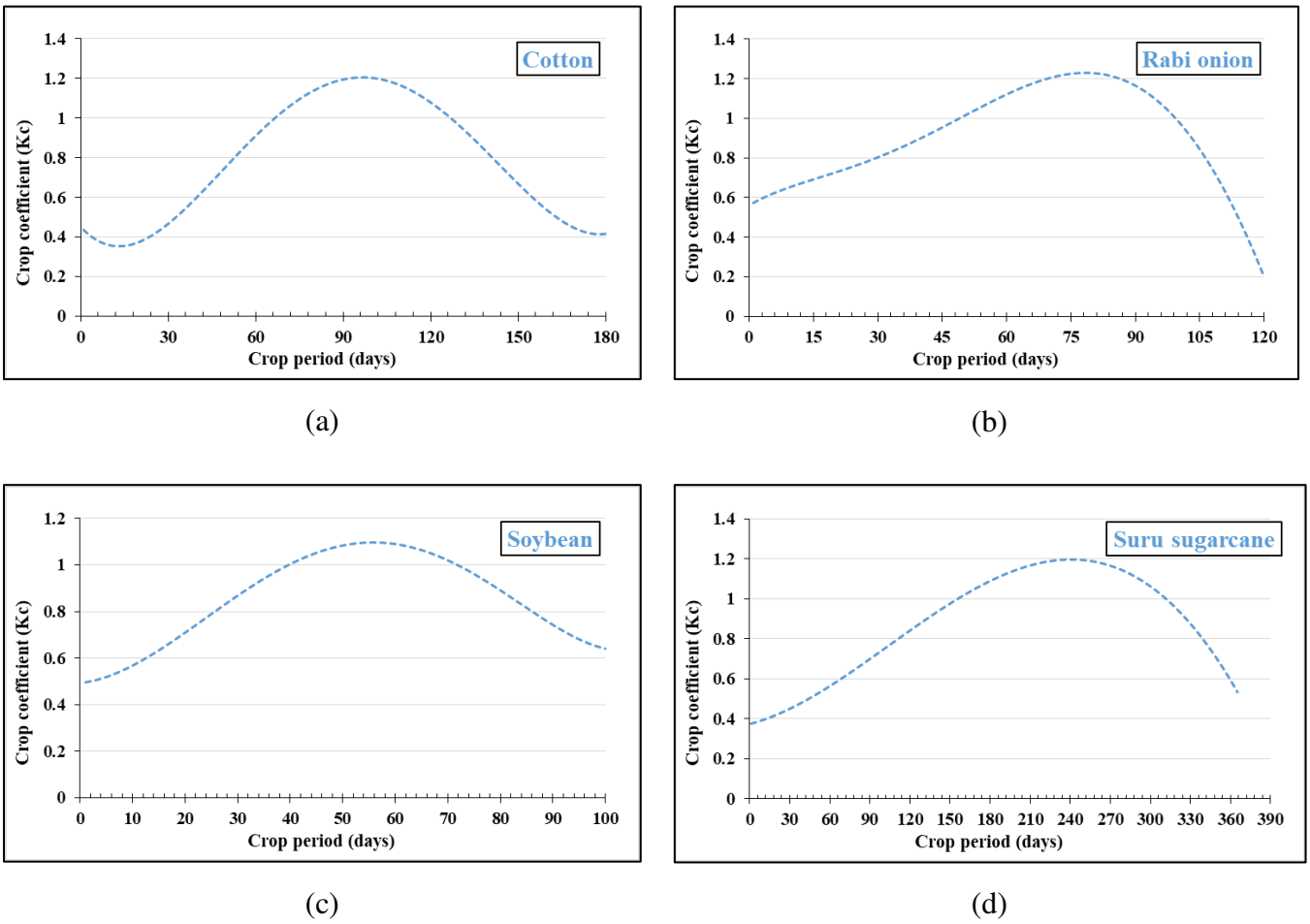

Fig. 2. Crop coefficient K_c curve during growth stage for a) Cotton, b) Onion, c) Soybean, and d) Sugarcane

2.5. Estimation of Future Crop Water Requirement

General circulation models (GCMs) can very well predict the significant characteristics of projected climate on a wide scale in the study of regional climate change. However, GCMs have limited utility due to their poor spatial resolution and lack of regional climate information. There are two ways in compensating for GCM's inadequacy in projecting regional climate change: one is to create new GCMs with higher resolution, and the other is to downscale GCMs to the regional scale. DownScaling techniques are categorized further as Dynamical DownScaling and Statistical DownScaling. Dynamical DownScaling is actually to build a regional climate model having a clear physical meaning and will not be affected by the observation data. However, it also has some disadvantages. For example, the requirement of significant computing resources and not readily transferred to new regions or domains. Statistical downscaling is premised on the theory that the large-scale climatic state and local physiographic factors influence regional climate (Zhou et al. 2017).

The SDSM developed by R. L. Wilby and C. W. Dawson started its life in the summer of 2000. It is the combination of multiple linear regression (MLR) and stochastic weather generator (SWG) (Wilby et al. 2002). MLR is used to build an empiric relationship between predictors (NCEP) and predictand (observed

local scale data) and develop regression parameters. A stochastic weather generator (SWG) simulates up to 100 daily time series from predictors of NCEP and GCMs based on the regression parameters (Mahmood and Babel 2013).

3.6 Theoretical Consideration of SDSM

SDSM (Statistical DownScaling Model) is a decision support method for evaluating local climate change impacts using a rigorous statistical downscaling approach. In addition, the program performs ancillary tasks of predictor variable pre-screening, model calibration, basic diagnostic testing, statistical analyses, and graphing of climate data.

The statistical downscaling technique utilized in this study was SDSM version 4.2 (Wilby and Dawson 2007) to simulate crop evapotranspiration for future periods centered on the 2030s, 2050s, and 2080s period. The step-by-step procedure using SDSM is summarized further.

The National Center for Environmental Prediction (NCEP) relates the intensity of each predictor-predict relationship, calibration and validation stage facilitates the establishment of statistical relationships between the selected predictors and the surface predictand (Gagnon et al. 2005). In this process, simulation of observed data was done with predictors from the re-analysis NCEP data, while for the 2030s, 2050s, and 2080s global climate model, HADCM3 with emission scenarios H3A2 and H3B2.

Table 4 Climatic scenario classes

Scenario Classes	Concerns	Remarks
A2	• Rapid economic growth • Low population growth • Rapid new technology • Concern to wealth rather than environment	• Homogenous world on economic development • Cultural convergence • No difference in per capita income
B2	• Diverse technological change • Emphasis on community initiative • Concern on environment rather than economic development	• Heterogeneous world • Local solutions for environmental and social sustainability

The IPCC has grouped future emission scenarios as four major classes/groups: a) A1, b) A2, c) B1, and d) B2 based on the level of economic development and environmental concern. It is to be observed (Table 4) that scenario group or class A2 is concerned more about activities that will improve the economic development of the world while, B2 is concerned more about the environmental sustainability of the world (Mohan and Ramsundram 2014).

Table 5 Details of predictors used in the present study

Sr. No	Predictor	Description
1	p_f	Surface airflow strength
2	p_u	Surface zonal velocity
3	p_v	Surface meridional velocity
4	p_z	Surface velocity
5	p_th	Surface wind direction
6	p_zh	Surface divergence
7	rhum	Surface relative humidity
8	p5_f	500 hPa airflow strength
9	p5_u	500 hPa zonal velocity
10	p5_v	500 hPa meridional velocity
11	p5_z	500 hPa vorticity
12	p5th	500 hPa wind direction
13	p5zh	500 hPa divergence
14	r500	500 hPa relative humidity
15	p8_f	850 hPa airflow strength
16	p8_u	850 hPa zonal velocity
17	p8_v	850 hPa meridional velocity
18	p8_z	850 hPa vorticity
19	p8th	850 hPa wind direction
20	p8zh	850 hPa divergence
21	r850	850 hPa relative humidity
22	p500	500 hPa geopotential height
23	p850	850 hPa geopotential height
24	temp	Mean temperature at 2m height
25	shum	Surface-specific humidity
26	mslp	Mean sea level pressure

The GCM outputs used in the analysis are derived from the United Kingdom Meteorological Office Hadley Centers Coupled Ocean/Atmosphere Climate Model, version 3 (HadCM3). It includes A2 (high greenhouse gas emissions) and B2 (low greenhouse gas emissions) scenarios with daily time series from 1961 to 2099. Similarly, the NCEP reanalyzed dataset is a daily time series from 1961 to 2000, including 26 large-scale weather factors. Table 5 represents the variable number, the abbreviation, and the description of the 26 GCM or NCEP weather factors.

The downscaling process involved the following steps; quality check of data, the transformation of data, screening of predictors, calibration of sub-model using observed data (predictand) and selected NCEP predictors, generation of present and future scenarios from gridded datasets of NCEP and GCMs, and statistical analysis.

2.5.1. Quality Control Check and Transformation of Observed Data (Predictand)

The meteorological stations might have anomalies or missing records following this quality control check function verifies the dataset. The missing data is replaced with the identifier value/code, i.e.-999. The second step after the quality control check is the transformation of data. SDSM can convert data before calibration in various formats such as logarithm, power, inverse, binomial, etc.(Saraf and Regulwar 2016).

2.5.2. Selection of Large-Scaled Predictor

The selection of predictors is a crucial step in the statistical downscaling process. The selection of predictors is governed by there four rules (Amin et al., 2014; Guo et al., 2018) stated below: (Amin et al. 2014; Guo et al. 2018) as below:

(1) There is a clear physical link between predictor and predictand.
(2) There is a strong correlation and agreement between predictor and predictand.
(3) The selected predictor can be simulated by the GCM.
(4) The selected predictors should maintain independence or at worst weak dependence.

The predictors of the SDSM model were chosen by screening of predictor variables. Correlation analysis, scatter plots, and seasonal variance methods of the SDSM model were used to screen the predictors that were strongly associated/correlated with the predictand. The number of control predictors in the recursive algorithm adopted by SDSM is limited to 12, while the predictors in GCM or NCEP are typically more than 20, making the correlation screening analysis more complicated and difficult to perform in one stage. After the selection of the large-scaled predictor, the selected predictors from the reanalysis data (NCEP) and predictand (observed station) data were used to establish the statistical relationships for the study area

2.5.3. Calibration and Validation of Model

Based on the available observed daily data, dataset was used in the calibration and validation of ET_0. The model was developed based on the selected NCEP predictors using monthly sub model. Unconditional sub model was used without transformation, and optimization of the best fit by ordinary least square (OLS).

The developed model for the ET_0 was simulated using NCEP, H3A2, and H3B2 predictors for 1968-2000, 1970-2000, and 1975-2000 for Solapur, Pune, and Rahuri station respectively as per availability of data. A total of 20 ensembles were generated using the annual and monthly SDSM and the mean of these ensembles was used in this study (Mahmood and Babel 2013). SDSM have the capacity to generate up to

100 ensembles and can be used to research the uncertainty analysis of climate scenario (Saraf and Regulwar 2016). 2/3rd of the total data was used for calibration and 1/3rd of the remaining data was used for validation. The calibration period for Pune, Rahuri, and Solapur were 1970- 1990, 1975-1990, and 1968-1989 respectively. Whereas, the validation period for Pune, Rahuri, and Solapur were 1991-2000, 1991-2000, and 1990-2000 respectively.

2.5.4. Statistical analysis for model performance

The mean (μ), coefficient of determination (R^2), nash-sutcliffe evaluation (E_{ns}), root mean square error (RSME), standard deviation (SD), standard error in mean (SE- μ), mean absolute deviation (MAD) and mean absolute percentage error (MAPE) for all three stations during the calibration and validation were used to evaluate the performance of SDSM (Huang et al. 2011; Mahmood and Babel 2013). The general equation of all statistical terms are described below.

(1) Coefficient of determination (R^2)

The coefficient of determination was used to show the accuracy of the model in predicting data. The coefficient of determination (R^2) is presented in.

$$R^2 = \frac{\sum(X_i - X') * (Y_i - Y')}{\sqrt{\sum(X - X')^2 * (Y - Y')^2}} \quad \text{.... (5)}$$

The value of R^2 explains the correlation between observed and downscaled values and lies between 0 and 1, where 0 indicates poor and 1 for the best.

(2) Nash-Sutcliffe evaluation (E_{ns})

Nash-Sutcliffe (E_{ns}) evaluation index (Eq. 9) was used to assess the model applicability by comparing observed data with output of SDSM.

$$E_{ns} = 1 - \frac{\sum_{i=1}^{n}(X_i - Y_i)^2}{\sum_{i=1}^{n}(X_i - X')^2} \quad \text{.... (6)}$$

X_i, and Y_i are time-series of observed value X and simulated value Y; and X', Y' are mean of observed value X and simulated value Y. Nash-Sutcliffe (E_{ns}) index ranges from $-\infty$ to 1, the closer the model efficiency is to 1, the more is accuracy (Guo et al. 2018).

(3) Root Mean Square Error (RMSE)

The Root Mean Square Error (RMSE) is a measure of difference between values predicted by a model and the values actually observed from the environment that is being modeled.

$$RMSE = \sqrt{\frac{\sum_{i=1}^{n}(X_{obs,i} - Y_{mod,i})^2}{n}} \quad \text{.... (7)}$$

Where $X_{obs,i}$ are observed value and $Y_{mod,i}$ are projected modelled value.

(4) Mean Absolute Percentage Error (MAPE)

The Mean Absolute Percentage Error (MAPE) is a measure of prediction accuracy of a forecasting method. It measures the size of the error in percentage terms. The statistical formula of MAPE is given in Eq. 11.

$$MAPE = 100 * \frac{1}{n} * \sum_{i=1}^{n} \left| \frac{X_i - Y_i}{X_i} \right| \quad \text{.... (8)}$$

Where X_i and Y_i are individual values of observed and modelled data respectively.

(5) Mean Absolute Deviation (MAD)

The Mean Absolute Deviation (MAD) of a data set is the average distance between each data value and the mean. Mean absolute deviation is a way to describe variation in a data set. The statistical formula of MAPE is given in Eq. 12.

$$MAD = \frac{\sum |(X - X')|}{n} \quad \text{.... (9)}$$

(6) Standard Error Mean (SE- μ) and Standard Deviation (SD)

The Standard Error in mean (SE- μ) was used to observe the variability of the data predicted by the model and was given by Eq. 13. The Standard Deviation (SD) is a measure of variability or the scatter or the dispersion about the mean value. It is given by the following Eq. 14.

$$SE = \sqrt{\frac{\sum_{i=1}^{n} (Y' - X')^2}{n}} \quad \text{.... (10)}$$

Where *n* is the number of time series and other notation same as above.

$$SD = \sqrt{\frac{\sum_{I=1}^{N} (X_i - X')^2}{N}} \quad \text{.... (11)}$$

Where, *Xi* is variable, *X'* is mean, and N is total number of variables

2.5.5. Generation of Present and Future Time Series for Reference crop evapotranspiration (ET_0)

Following calibration and validation of model, weather generator function was applied to generate assembles of synthesis daily time series of ET_0 presenting climate from selected set of NCEP predictors. The generated daily time series of ET_0 was compared statistically with the observed records to check how close it was to the present climate. Finally, the scenario generator function was used to stimulate future time series of ET_0 using output from GCMs (HadCM3) under H3A2 and H3B2 scenarios.

Daily ET_0 data of the observed period for the mentioned stations was provided in (.DAT) format to SDSM model, and the model input files have been established in accordance. The downscaled data as per

requirements was simulated for three future periods based on base period. As discussed earlier, downscaling was done for three time periods 2030s, 2050s and 2080s depending on the observed data period

Considering, Solapur station: The observed data was available for 33 years. The years were split as (16 +1 + 16) where, first 16 is considered as pre years and next 16 as post years. Thus, the analysis period for 2030s was 2014 – 2046 keeping year 2030 at centre. The similar procedure was adopted for 2050s, 2080s and for remaining stations (Table 6).

Table 6 Analysis period/time for projecting future scenarios in ET_0

Periods	**Solapur**	**Pune**	**Rahuri**
Base/Observed Period	1968 – 2000	1970 – 2000	1975 – 2000
First period (2030s)	2014 – 2046	2015 – 2045	2017 – 2043
Second period (2050s)	2034 – 2066	2035 – 2065	2037 – 2063
Third period (2080s)	2064 – 2096	2065 – 2095	2067 – 2093

The steps involved in downscaling and scenario generation is shown in Fig. 3.

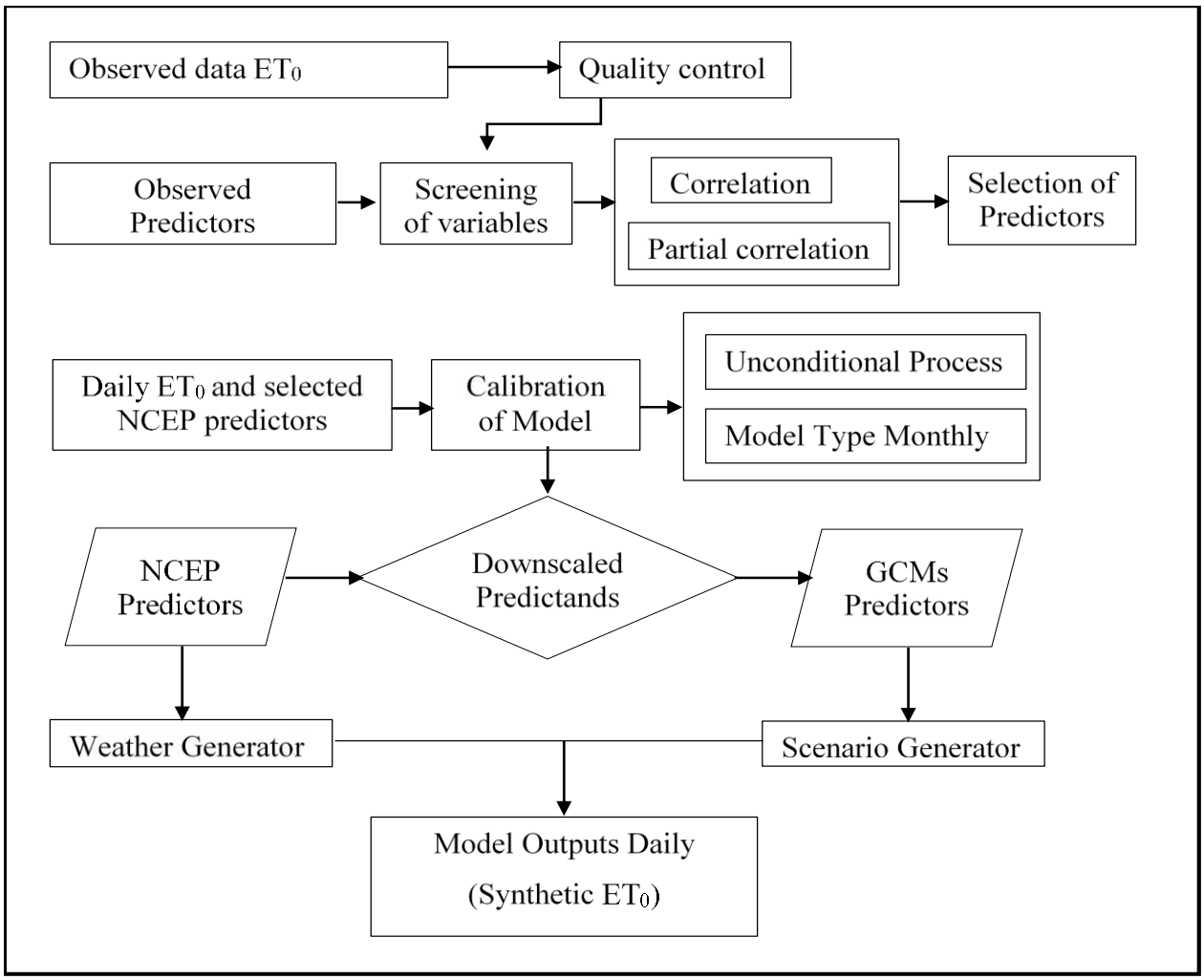

Fig. 3. Flow chart showing depicting involved during downscaling and scenario generation modified after (Wilby and Dawson 2007; Saraf and Regulwar 2016)

3. Results

The study was undertaken to analyze variability in crop water requirements for future atmospheric conditions. The daily ET_0 was calculated using the Penman-Monteith equation as discussed in section 2.4. The output of daily ET_0 was used for projecting future ET_0 during different periods. The projected ET_0 in combination with crop coefficient (Kc) calculated CWR for future periods, and further variation in crop water requirement was analyzed using observed data. Based on base climate data, the SDSM was used to project future ET_0 for three periods the 2030s, 2050s, and 2080s. The results of the analysis were presented separately for Pune, Rahuri, and Solapur stations. The performance of SDSM model predictions was studied using observed and predicted values of ET_0 during the same period.

3.1. Screening of predictors

The selection of predictors was a crucial step in the downscaling process. It is an iterative procedure consisting of a rough screening of the predictors repeated until an objective function is optimized (Wilby and Harris 2006). The variables with the highest correlation were selected using the screen variable tool in the SDSM. Initially, all the predictors from historical records were correlated with the observed data of ET_0. The predictors with the highest correlation were chosen with (minimum or zero) p-value and (maximum) partial r value. The correlation statistics and p-values explain the strength of the relationship between the predictor–predictand and multi co-linearity among selected predictors. The number of selected predictors varied from three to four. To have better prediction results, all correlations with a p-value (<= 0) were selected. Table 7 represents the selected predictors along with the partial r value for ET_0.

Table 7 Selected predictors with partial r values for reference crop evapotranspiration (ET_0)

Sr. No.	Predictors	Meteorological stations with partial r values					
		Pune		Rahuri		Solapur	
1	nceptempas	✓	0.494	✓	0.362	✓	0.337
2	ncepp_zhas			✓	0.260	✓	0.245
3	ncepp_uas	✓	0.185	✓	0.243		
4	ncepp5_uas	✓	0.244				
5	ncepp8_uas					✓	0.101
6	ncepp8_vas			✓	0.124	✓	0.056

(Suo et al. 2019) examined partial r values for temperature in the range of 0.27 to 0.77. Similarly, identical partial r values for temperature and precipitation were also observed by Mahmood and Babel, 2013. The highest correlation values represent a higher degree of association, while smaller p-values describe a better chance of association between variables. The selection of predictors was done as discussed in section 2.5.2. Amongst 26 predictors, only six (nceptempas, ncepp_zhas, ncepp_uas, ncepp5_uas, ncepp8_uas, and ncepp8_vas) were used as they strongly correlated with observed (ET_0) (Table 7). For all three weather

stations, nceptempas (the temperature at 2m height) was super predictor and common to three stations with the highest 'partial r' value. A similar super-predictor (nceptempas) in downscaling of ET_0 for nine stations in the Beijing region was also examined by (Guo et al. 2018).

3.2. Calibration and Validation of Model

The Calibrate Model operation takes a user-specified predictand with a set of predictor variables and computes the parameters of multiple regression equations via an optimization algorithm (ordinary least squares). Prior to future scenario construction, the results of the observed data of ET_0 were correlated with the modeled data during the calibration and validation. All measured statistical values were conspicuously resembling the statistics of observed data for ET_0.

Table 8 Statistical criteria for best fit model for downscaling ET_0 during calibration for HadCM3 model

Pune (1970-1990)								
Data type	**R^2**	***E_{ns}***	**RMSE**	**MAPE**	**μ**	**S.D.**	**SE-μ**	**MAD**
OBS	-				4.583	1.39	0.016	1.38
NCEP	0.71	0.713	0.92	16.10	4.575	1.05	0.012	1.21
H3A2	0.72	0.719	0.91	16.12	4.584	1.07	0.012	1.22
H3B2	0.72	0.721	0.90	16.09	4.574	1.06	0.012	1.23
Rahuri (1975 – 1990)								
Data type	**R^2**	***E_{ns}***	**RMSE**	**MAPE**	**μ**	**S.D.**	**SE-μ**	**MAD**
OBS	-				5.087	1.47	0.019	1.44
NCEP	0.69	0.685	1.000	15.86	5.073	1.10	0.014	1.23
H3A2	0.68	0.683	1.003	15.93	5.080	1.12	0.015	1.24
H3B2	0.68	0.683	1.002	15.84	5.078	1.13	0.015	1.24
Solapur (1968- 1989)								
Data type	**R^2**	***E_{ns}***	**RMSE**	**MAPE**	**μ**	**S.D.**	**SE-μ**	**MAD**
OBS	-				5.709	1.73	0.019	1.61
NCEP	0.60	0.603	1.32	18.33	5.689	1.27	0.014	1.39
H3A2	0.61	0.609	1.31	18.19	5.690	1.25	0.014	1.39
H3B2	0.61	0.609	1.31	18.16	5.694	1.27	0.014	1.38

The SDSM showed the best values of all performance measures, higher values for R^2 and E_{ns} and lower values for RMSE and MAPE. The MAD values confront that there was consistently less variation among observed and downscaled data ranged from 1.2 to 1.6 mm. The analysis also pointed out that the performance measures as R^2 and E_{ns} were more than 0.71, 0.68, 0.60 for Pune, Rahuri, and Solapur stations, respectively. The values of RMSE varied from 0.90 to 0.92 for Pune, 1.000 to 1.003 for Rahuri, and 1.31 to 1.32 mm for Solapur station.

Similarly, it was worth noticing that for calibration, MAPE was less than 16.12, 15.93, and 18.33 % for Pune, Rahuri, and Solapur stations, sequentially. The mean, standard deviation, and standard error mean

suggested that observed and modeled data had an almost similar mean, lesser deviation, and lesser error between observed and predicted values.

Table 9 Statistical criteria for best fit model for downscaling ET_0 during validation for HadCM3 model

Pune (1991-2000)								
Data type	**R^2**	***E_{ns}***	**RMSE**	**MAPE**	**μ**	**S.D.**	**SE-μ**	**MAD**
OBS	-				4.452	1.62	0.027	1.30
NCEP	0.70	0.698	0.89	15.96	4.442	1.38	0.023	1.15
H3A2	0.70	0.698	0.89	15.78	4.434	1.39	0.023	1.16
H3B2	0.70	0.701	0.88	15.68	4.442	1.40	0.023	1.16
Rahuri (1991 – 2000)								
Data type	**R^2**	***E_{ns}***	**RMSE**	**MAPE**	**μ**	**S.D.**	**SE-μ**	**MAD**
OBS	-				4.221	1.44	0.024	1.17
NCEP	0.71	0.71	0.78	14.48	4.201	1.22	0.020	0.98
H3A2	0.70	0.70	0.79	14.51	4.211	1.23	0.020	0.99
H3B2	0.71	0.71	0.78	14.37	4.196	1.24	0.020	1.00
Solapur (1990- 2000)								
Data type	**R^2**	***E_{ns}***	**RMSE**	**MAPE**	**μ**	**S.D.**	**SE-μ**	**MAD**
OBS	-				4.850	1.67	0.026	1.35
NCEP	0.62	0.61	1.11	18.51	4.842	1.37	0.022	1.14
H3A2	0.62	0.61	1.12	18.56	4.849	1.36	0.021	1.15
H3B2	0.61	0.61	1.10	18.43	4.836	1.36	0.021	1.15

Similarly, statistical performance during the validation period is represented in Table 9. In the Rahuri station, considering NCEP data, the value of the R^2 and *Ens* was 0.71 in the validation stage. There were lesser values of RMSE and MAPE as 0.78 and 14.48, respectively. An identical closer difference during the calibration and validation period for each performance measure of the remaining data of HadCM3 (H3A2 and H3B2 scenarios) for Pune and Solapur stations.

Overall, the performance suggested that for the accurate projection of ET_0, HadCM3 data is a valid approach. Based on the results of Table 8 and Table 9, the derived predictor–predictand relationships were considered satisfactory for three stations. (Guo et al. 2018) observed that the value of R^2 and *Ens* ranged from 0.61 to 0.78 during calibration and validation of downscaled ET_0 in China. Similar values of R^2 were also observed by (Saraf and Regulwar 2016) during calibration of observed and modeled temperature for the Godavari basin, Maharashtra (India)

3.3. Projected Changes in ET_0 for Future Climate Scenarios

The changes of mean monthly ET_0 in the three selected stations under all scenarios would present noticeable differences in different months.

3.3.1. Future projections and percent change in ET_0 for Pune station

Fig. 4a and b represented the changes in ET_0 for future 2030s, 2050s, and 2080s relative to the base period (1970–2000) under H3A2 and H3B2 scenarios for Pune stations. The figure represents general monthly changes observed in modeled ET_0. It depicted that the changes in ET_0 projected under both scenarios were quite different in magnitude (amount) but identical in pattern. The maximum mean monthly ET_0 (7.43 mm) for the base period was observed in May whereas, the minimum ET_0 was 3.08 mm in December. Projected ET_0 presented an increasing trend in the entire period from 2015 to 2095 under both scenarios during the 2030s, 2050s, and 2080s. The maximum projected ET_0 would be in May followed by April during the 2030s, 2050s, and 2080s whereas, the minimum projected ET_0 would be in December followed by August.

During the 2050s and 2080s periods, there would be an increment in the average ET_0 for all months except June and August. The maximum decrease in mean monthly ET_0 for the 2050s would be in August (-9.15 %) under the H3A2 and -8.78 % under the H3B2 scenario. In the 2080s, ET_0 in August would be moderated by -3.81 and -7.36 % under H3A2 and H3B2 scenarios, respectively observed in Fig. 4c and d.

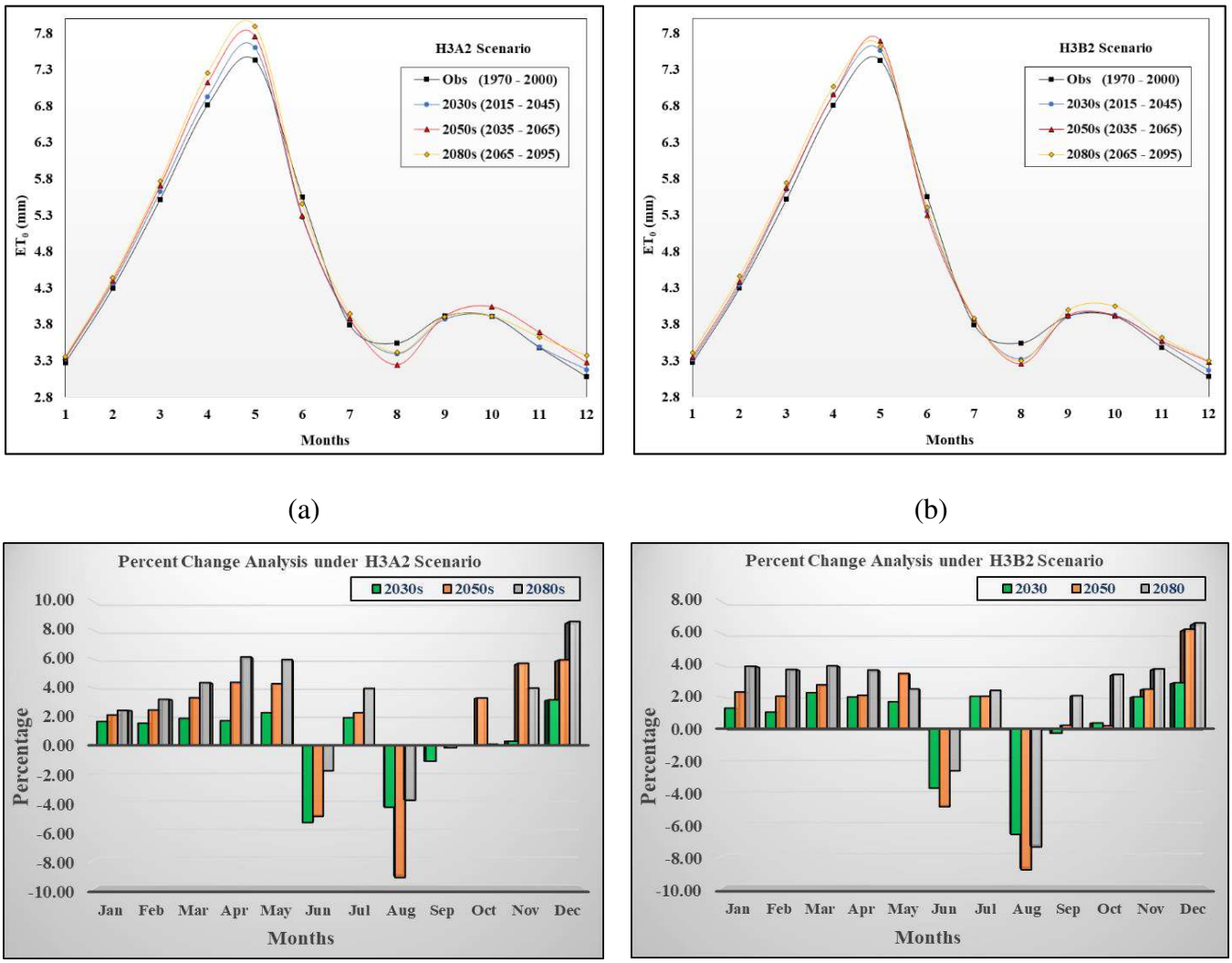

Fig. 4. Mean monthly downscaled ET_0 under (a) H3A2 and (b) H3B2 scenario; and percent changes in ET_0 as compared to base period under (c) H3A2 and (d) H3B2 scenario for Pune station

3.3.2. Future projections and percent change in ET_0 for Rahuri station

ET_0 constantly advanced over three periods at Rahuri station with a maximum increasing rate in contrast to the baseline period, computed for the 2080s. The max and min mean monthly ET_0 during the base period was observed in May (7.54 mm) and Dec (2.98 mm), respectively. The maximum projected ET_0 during the 2030s, 2050s, and 2080s would be in May followed by April month whereas, the minimum projected ET_0 would be in Dec followed by Nov month Fig. 5a and b

The percentage change in ET_0 for Rahuri station revealed variation in the range for 2030s (-3.24 to 5.04%), 2050s (-4.73 to 5.59%), and 2080s (-5.96 to 12.39%) under H3A2 scenario whereas, in the range for 2030s (-4.91 to 4.92%), 2050s (-6.40 to 7.23%), and 2080s (-6.49 to 8.52 %) Fig. 5c and d. (Kundu et al. 2017) observed increase in projected ET_0 with fluctuation of both increase and decrease during different decades with the highest rise projected in period 2091–2099, particularly in the winter season from Nov to Jan.

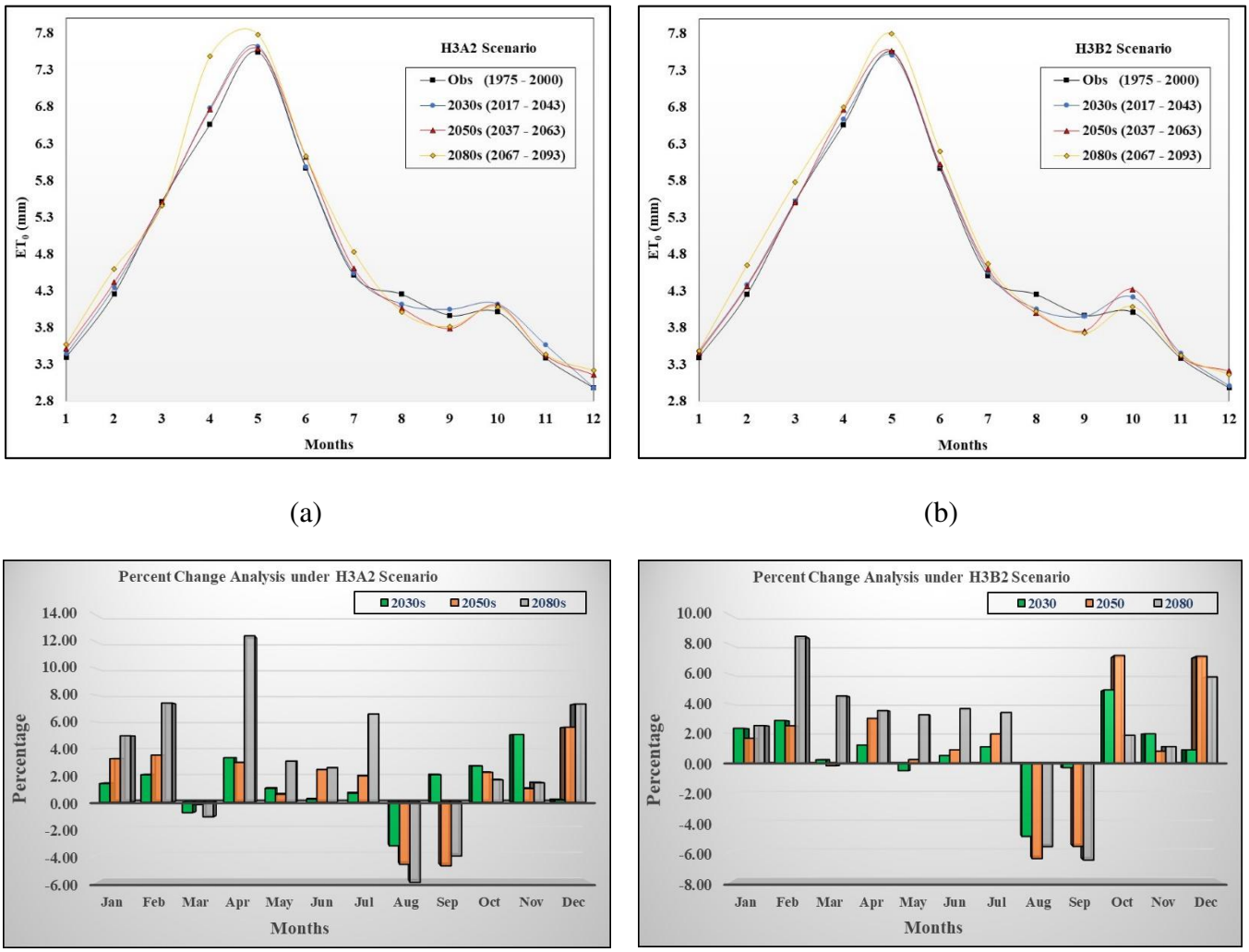

Fig. 5. Mean monthly downscaled ET_0 under (a) H3A2 and (b) H3B2 scenario; and percent changes in ET_0 as compared to base period under (c) H3A2 and (d) H3B2 scenario for Rahuri station

3.3.3. Future projection and percent change in ET_0 for Solapur station

Solapur station had higher mean monthly ET_0 values for all months as compared to Rahuri and Pune station. The maximum and minimum mean monthly ET_0 during the base period was in May (8.25 mm) and Dec (3.90 mm), respectively Fig. 6a and b. The maximum projected ET_0 under both scenarios during the 2030s, 2050s, and 2080s would be in May followed by April whereas, the minimum ET_0 would be in Dec followed by Nov. The mean annual ET_0 for Solapur station during the observed period is 5.41 mm, and ET_0 would show increment with 1.76, 2.01, and 2.73 % under the H3A2; and 1.54, 2.52, and 3.13 % under H3B2 scenario, during the periods of 2030s, 2050s, and 2080s respectively, Fig. 6 c and d.

Overall, it was envisioned a gradual rise in projected ET_0 during the 2030s, 2050s, and 2080s periods for most of the months. The maximum and minimum mean monthly projected ET_0 would be observed in May and December, respectively, under both scenarios (H3A2 and H3B2). The projected ET_0 during the 2030s, 2050s, and 2080s compared to the base period found decreased in June, Sept., and Oct. month under both

scenarios with maximum reduction in ET_0 examined in Sept.

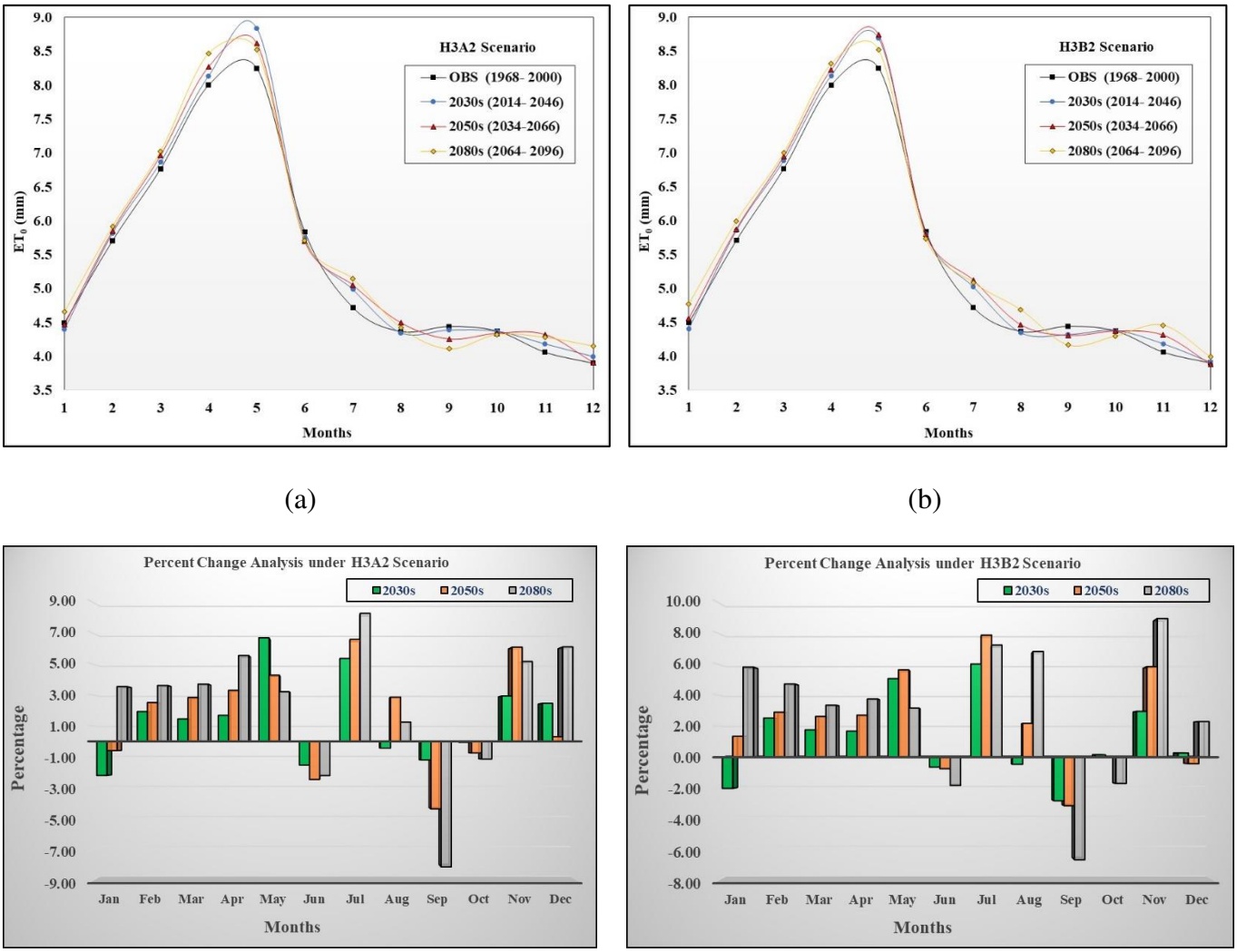

Fig. 6. Mean monthly downscaled ET_0 under (a) H3A2 and (b) H3B2 scenario; and percent changes in ET_0 as compared to base period under (c) H3A2 and (d) H3B2 scenario for Solapur station

3.4. Future Crop Water Requirement in Potential Climate Scenarios

Crop evapotranspiration (ETc) is closely correlated with ET_0. It indicates the quantity of water that a type of plant needs during the crop development phase. Considering, the projected ET_0 and present Kc values, the crop water requirement was estimated for cotton, onion, soybean, and sugarcane for three stations (Pune, Rahuri, and Solapur) for the 2030s, 2050s, and 2080s period. Owing to the varied growing periods and Kc values, the water requirements of the four crops were different. Crop water requirement was calculated for a three-time period considering both H3A2 and H3B2 scenarios.

3.4.1. Cotton

The predicted ET_0 in the earlier section considering both scenarios revealed that reference evaporation (ET_0) increased for all months except June to Sept (Kharif Season). Therefore, it is obvious that the water

requirement of cotton would decrease or most likely be the same as that of the base period. Fig. 7 represents the variation in CWR of cotton during different periods for all three stations. The base period water requirement of cotton for the Pune station is 620.2 mm. The CWR would marginally decrease during the 2030s and 2050s as compared to the present condition. The marginal increase in CWR would be observed in the 2080s over a base period with 626.1 mm under H3A2 and 622.1 mm under H3B2 scenarios for the Pune station. For Rahuri station, the base period CWR is 672.3 mm and, it would relatively increase with 4.8 mm and 4 mm for the 2030s and 2080s period, respectively, and found a relative decrease during 2050s (-4.5 mm) under the H3A2 scenario. The Solapur station witnesses' a higher CWR (717.6 mm) for a base period compared to Rahuri and Pune station. The CWR for Solapur station would increase during all three periods under both scenarios. (Doria et al. 2006) compared results of estimated CWR to the base period and observed an increase in CWR by 3.0 % (20 mm) per season for the 2020s and about 7.0 % (43 mm) per season for 2050s using both H3A2 and H3B2 scenarios.

Overall, it was concluded that the CWR of cotton would be approximately the same (less than 1% variation) during the periods the 2030s, 2050s, and 2080s concerning the base period for Pune and Rahuri station, whereas marginally increase (0.91 to 2.48% variation) for all periods at Solapur station.

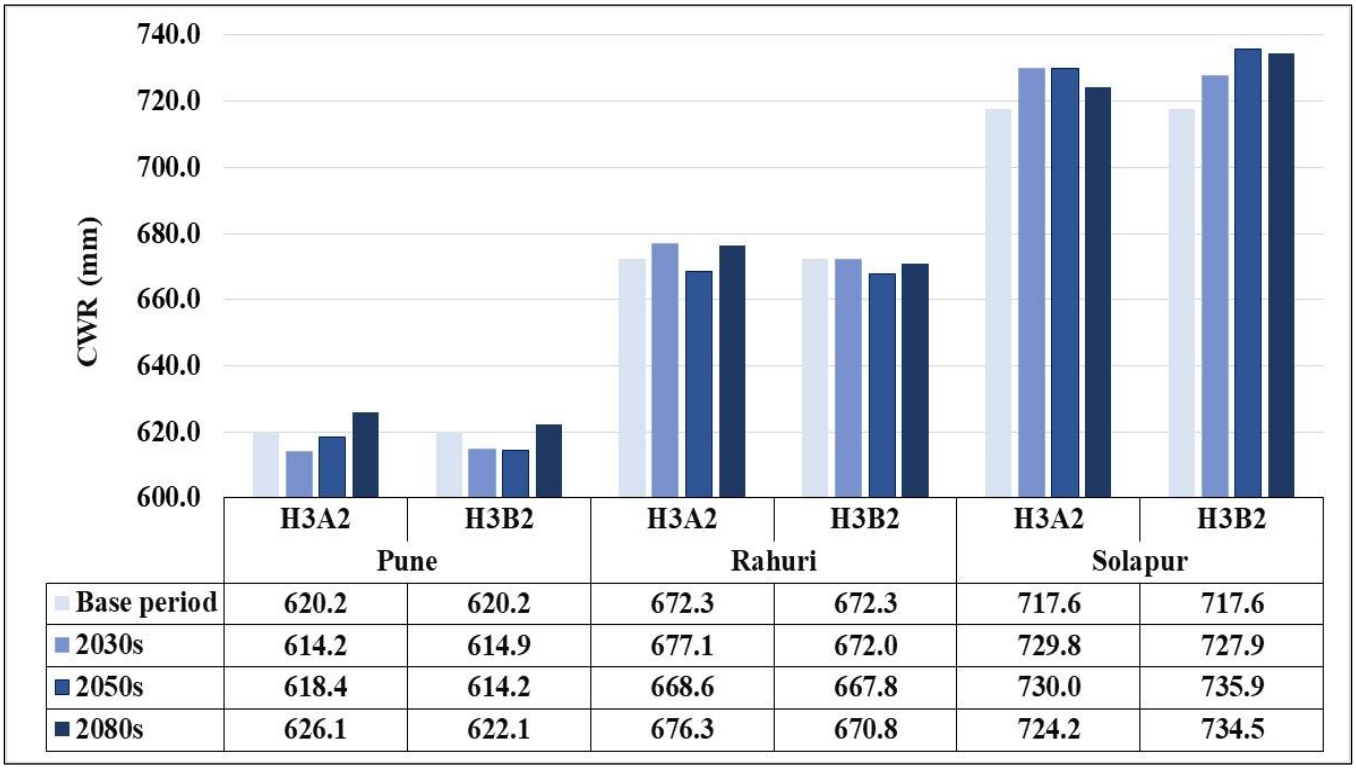

	Pune		Rahuri		Solapur	
	H3A2	H3B2	H3A2	H3B2	H3A2	H3B2
Base period	620.2	620.2	672.3	672.3	717.6	717.6
2030s	614.2	614.9	677.1	672.0	729.8	727.9
2050s	618.4	614.2	668.6	667.8	730.0	735.9
2080s	626.1	622.1	676.3	670.8	724.2	734.5

Fig. 7. CWR of cotton during different time period at different stations

3.4.2. Onion

The base/observed period CWR of onion for the Pune station is 428.9 mm. The CWR would relatively increase by 6.3, 18.1, and 17.9mm under the H3A2 scenario; and 7.1, 12.9, and 19.9mm under the H3B2 scenario during the 2030s, 2050s, and 2080s, respectively (Fig. 8). The increment in the CWR was due to

the increasing trend in ET_0 observed during the growth period Nov to Feb. Similarly, the base period CWR of onion for Rahuri is quite identical to Pune station (428.3 mm). The CWR would relatively increase in the 2030s as 437.9 and 429.2 mm under H3A2 and H3B2 scenarios, respectively. The CWR for Solapur station would marginally increase during the 2030s and found a relatively increase during 2050s under both scenarios. In the 2080s period, the CWR of onion would increase as 559.1 mm by 21 mm under H3A2 and 562.1 mm by 24 mm under H3B2 sequentially.

The CWR would advance for all three stations during the 2030s, 2050s, and 2080s. It would marginally increase (0.49 to 2.48 %) during the 2030s, whereas the 2050s and 2080s periods would observe the highest increment in CWR (1.80 to 4.62 %) for all three stations. The reason could be a predominant increase in the ET_0 during the winter season under both scenarios.

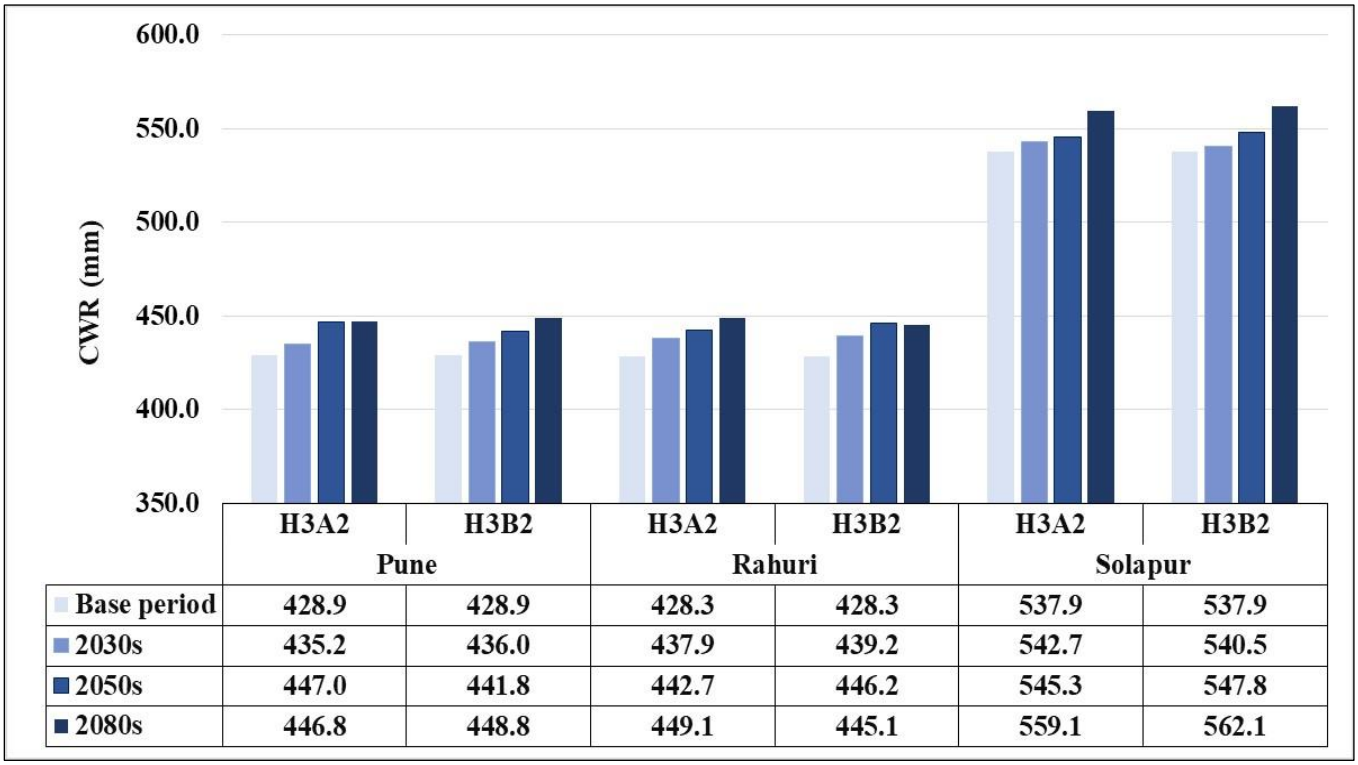

	Pune		Rahuri		Solapur	
	H3A2	H3B2	H3A2	H3B2	H3A2	H3B2
Base period	428.9	428.9	428.3	428.3	537.9	537.9
2030s	435.2	436.0	437.9	439.2	542.7	540.5
2050s	447.0	441.8	442.7	446.2	545.3	547.8
2080s	446.8	448.8	449.1	445.1	559.1	562.1

Fig. 8. CWR of *onion* during different time period at different stations

3.4.3. Soybean

Fig. 9 represented the changes in CWR of soybean during different periods for all three stations. For Pune station, the CWR under the H3A2 scenario would marginally decrease by -1.05, -1.05, and -0.16 % during the 2030s, 2050s, and 2080s, respectively. Similarly, CWR would show variation in the range (-1.67 to 0.06% %) compared to a base period under the H3B2 scenario. The Rahuri station corresponded to similar variation as Pune station with variation in the range as -2.09 to 0.37%. The CWR of soybean for Solapur station would marginally increase or approximately be the same during all three periods (the 2030s, 2050s, and 2080s) under both scenarios. The CWR would show an increment of up to 1.63% during the 2080s. (Manasa and Shivapur 2016) observed both rise and fall in CWR for the future scenario compared with a

base period with a decrease in CWR during Kharif crops (jowar, maize, groundnut, soybean, cotton) while, increase in CWR during rabi crops (sugarcane and wheat).

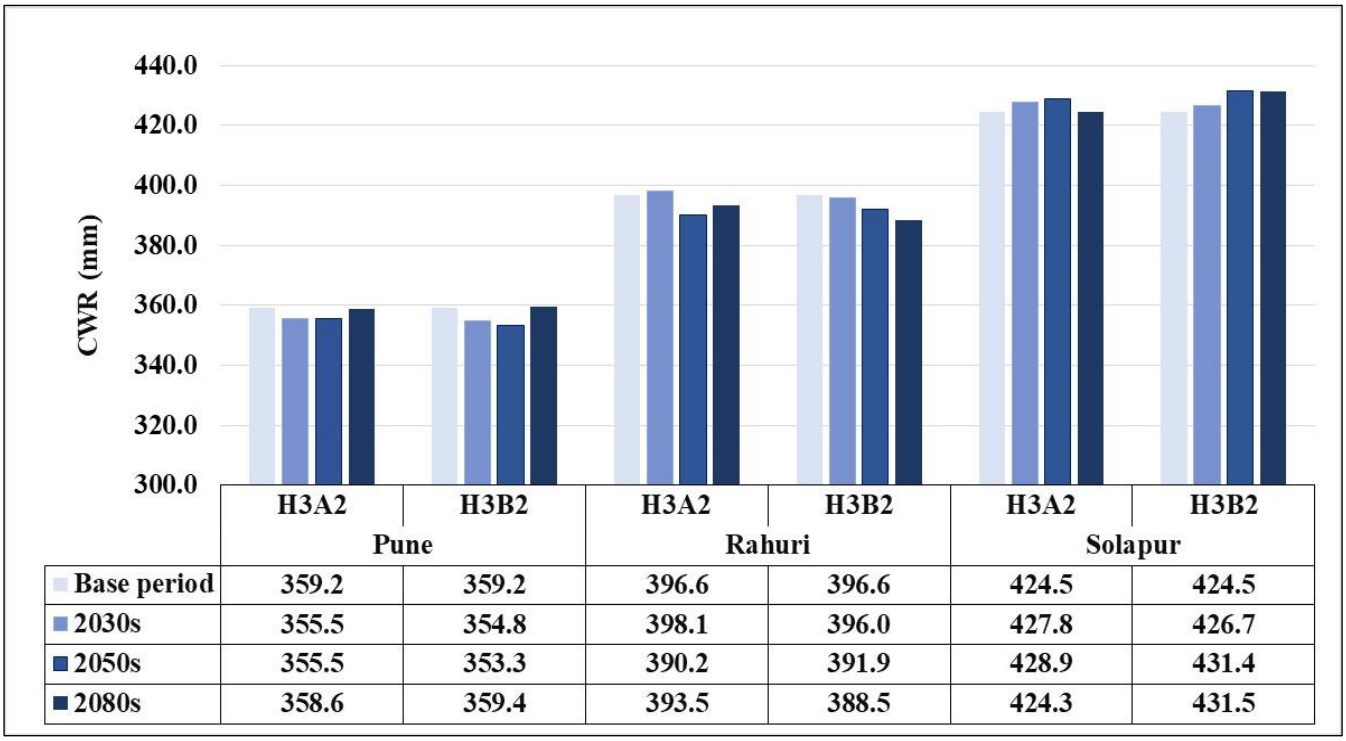

	H3A2	H3B2	H3A2	H3B2	H3A2	H3B2
	Pune		Rahuri		Solapur	
Base period	359.2	359.2	396.6	396.6	424.5	424.5
2030s	355.5	354.8	398.1	396.0	427.8	426.7
2050s	355.5	353.3	390.2	391.9	428.9	431.4
2080s	358.6	359.4	393.5	388.5	424.3	431.5

Fig. 9. CWR of soybean during different time period at different stations

3.4.4. *Sugarcane*

Sugarcane resembles the highest increase in crop water requirement as compared to cotton, onion, and soybean. The base/observed period CWR of sugarcane for the Pune station is 1384.6 mm. The highest increment in CWR of sugarcane would be during the 2080s, with estimated CWR values as 1421.4 and 1410.8 mm under H3A2 and H3B2 scenarios, respectively (Fig. 10). The CWR for Rahuri station would relatively increase in the 2030s as 1460.6 and 1452.8 mm under H3A2 and H3B2 scenarios, respectively.

The 2080s period could observe an increase by 41.1 mm and 24.8 mm under H3A2 and H3B2 scenarios, respectively, as compared to a base period. For Solapur station, CWR of sugarcane under the H3A2 would relatively increase during the 2030s (1.66 %) and 2050s (1.83 %); and increase during 2080s (2.26 %). Similarly, under the H3B2 scenario, the increment in CWR during the 2030s, 2050s, and 2080s would be 1.37, 2.37, and 2.86 %, respectively.

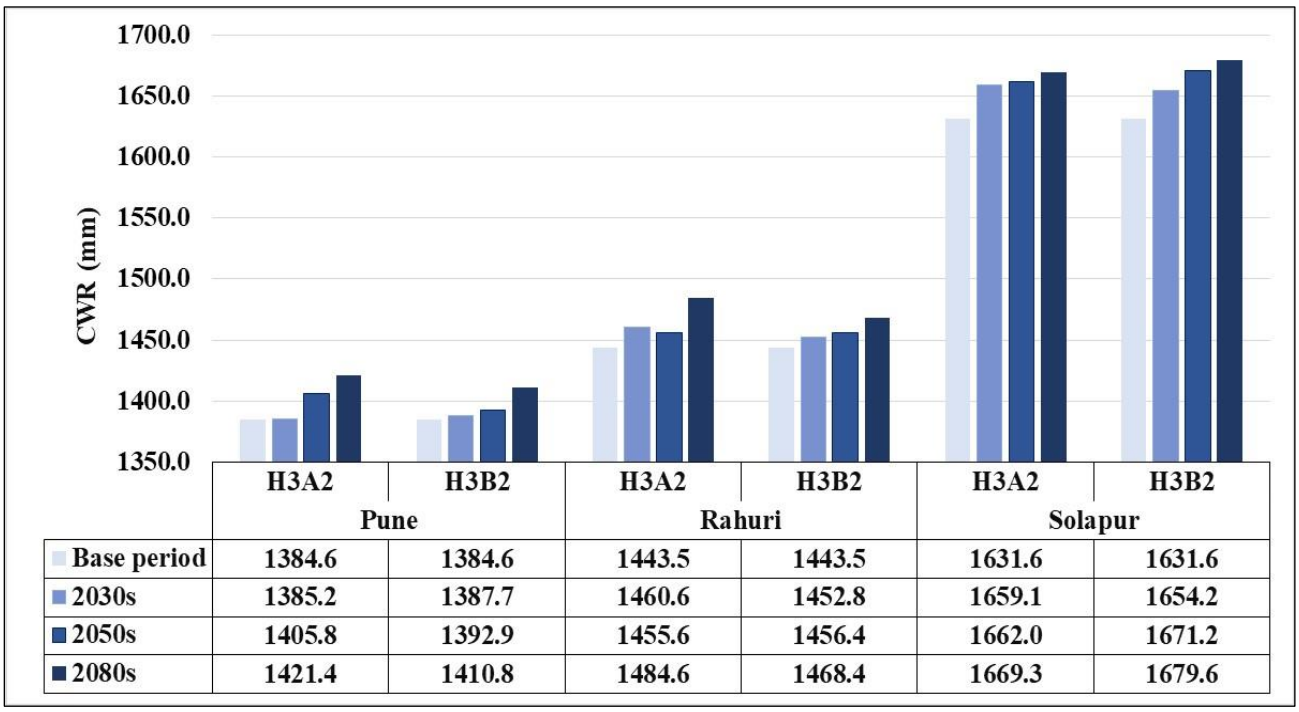

	H3A2	H3B2	H3A2	H3B2	H3A2	H3B2
	Pune		Rahuri		Solapur	
Base period	1384.6	1384.6	1443.5	1443.5	1631.6	1631.6
2030s	1385.2	1387.7	1460.6	1452.8	1659.1	1654.2
2050s	1405.8	1392.9	1455.6	1456.4	1662.0	1671.2
2080s	1421.4	1410.8	1484.6	1468.4	1669.3	1679.6

Fig. 10. CWR of *sugarcane* during different time period at different stations

4. Discussions

Western Maharashtra, located in the semi-arid zone of India, is a core region for the economic growth of Maharashtra state. The area has an arid climate, minimal water supply, and is one of the most fragile ecological environments in the country. The geographical area of the state of Maharashtra is 30.7 M-ha, and the cultivable area is 22.5 M-ha. Therefore a means to optimize water resources management to achieve sustainable development of the region, it is critical to explore the requirements for CWR. At the same time, it is also inevitable to estimate the crop coefficient (Kc) of different parts.

SDSM is used to downscale and project long-term (the 2030s, 2050s, and 2080s) future scenarios of ET_0 from predictors of HadCM3 models in the Western Maharashtra region, India. The H3A2 and H3B2 forcing emission scenarios generated future ET_0 series. The monthly SDSM sub-model is found effective in downscaling of ET_0. SDSM projects an increase in mean annual ET_0 for future periods under both scenarios. The relative changes in annual ET_0 range from 0.42 to 3.09%, 0.77 to 3.52%, and 1.54 to 3.13% for Pune, Rahuri, and Solapur stations, respectively. The highest increase in projected monthly ET_0 reached 8.57%, and the decrease approached -9.15% at Pune. Similarly, the maximum positive increment in projected monthly ET_0 reaches 12.39%, and the decrease is -6.49% at Rahuri station. As for Solapur station, the relative changes range from -8.09% to 8.93%, indicating a trend of increase concerning the projected climate change. The uncertainty in future ET_0 projections due to GCMs, emission scenarios, and different time stages is maximum.The results in section 3.3 of this paper show that despite an increasing trend in annual ET_0 during a future period, the ET_0 would drastically decrease in some months. The projected changes in ET_0 revealed that all months during three future periods (the 2030s, 2050s, and 2080s) showed an increment in ET_0

compared to a base period. The ET_0 would advance during summer, pre-monsoon, and winter seasons whereas, it could decrease during the monsoon (Kharif) season. This further implies a decrease in CWR of Kharif crops (cotton and soybean). The CWR would be equal to or less than that of the present condition. Alternatively, CWR of rabi crop (onion) shows a phenomenal increase of up to 4.62%. The perennial crop sugarcane corresponds marginal increase in water requirement in the range (0.05 to 2.86%).

Any of the shortcomings of this research may be the subjects of future investigations. Even though SDSM is a versatile tool in downscaling method, it does not have any physical significance, and the extent of parameter changes is unknown. Since ET_0 plays a vital role in the hydrological cycle, numerous studies have concentrated on researching ET_0 variability and analysed that ET_0 is shifting periodically (Chattopadhyay and Hulme 1997; Bandyopadhyay et al. 2009; Zeng et al. 2019). If there is a loop in CWR at this point, whether or not the future CWR will have the same cycle is not be taken into consideration. There is also a cascade of ambiguity in the climate change impact analysis, including uncertainty arising from GCMs, emission scenarios, the hydrological model, and the parameters (Wilby and Harris 2006; Xu et al. 2013).

However, it must be understood that such findings are very much based on the existence of potential climate forecasts and approaches to GCM used in this research. When large data is available a more sophisticated downscaling method should be used, as different methods will generate different future climate predictions (Chiew et al. 2010; Xu et al. 2013).

5. Conclusion

Many researchers have pointed out that fluctuations in ET_0 have dramatically shifted as climate change has been escalated. In the present study, we selected Western Maharashtra to analyze variability in CWR by downscaling ET_0. The SDSM performs satisfactorily in downscaling ET_0 with values more than 0.60 for R^2 and *Ens* and less than 1.32 and 18% for RMSE and MAPE, respectively, during calibration and validation periods. The projected changes showed an increase in ET_0 for all months (in summer, winter, and pre-monsoon seasons) and a decrease from June to September (monsoon season) during the 2030s, 2050s, and 2080s period compared to the base period under both H3A2 and H3B2 scenario. The result particularizes a decrease in projected CWR for Kharif season and an increase in CWR for rabi and summer season. The estimated future CWR showed variation in the range for cotton (-0.97 - 2.48%), soybean (-2.09 - 1.63 %), onion (0.49 - 4.62 %), and sugarcane (0.05 - 2.86 %) during the 2030s, 2050s, and 2080s period compared to present condition for Pune, Rahuri and Solapur stations under both H3A2 and H3B2 scenario. Looking at the impact of climate variability on crop water requirements there is a need to promote water-saving technologies like drip and sprinkler irrigation systems. Also, promote rain-water conservation and increase groundwater recharge in the Western Maharashtra region to minimize the risk of yield reduction and enhance maximum water availability in the study area due to climatic variability.

Declaration of Competing Interest

The authors declare that they have no known competing financial interests or personal relationships that could have appeared to influence the work reported in this paper. The authors did not receive support from any organization for the submitted work.

Data Availability

The data that support the findings of this study are available on request from the corresponding author 'Shubham Gade'. The data are not publicly available as they containing information that could compromise research participant privacy/consent.

Code Availability

No code is available for the present study.

Compliance with Ethical Standards

This article does not contain any studies with human participants or animals performed by any of the authors.

Consent to Participate

Informed consent was obtained from all individual participants included in the study.

Consent to Publish

The participant has consented to the submission of the article to the journal

Conflict of Interest

The author declares no conflict of interest.

Acknowledgments

We appreciate the editors and the reviewers for their constructive suggestions and insightful comments, which helped us to improve this manuscript.

References

Allen RG, Pereira LS, Raes D, Smith M (1998) Crop evapotranspiration-Guidelines for computing crop water requirements- FAO Irrigation and drainage paper No. 56. FAO, Rome. 91–165

Amin MZM, Islam T, A I (2014) Downscaling and projection of precipitation from general circulation model predictors in an equatorial climate region by the automated regression-based statistical method. Theor Appl Climatol 118:347–364. https://doi.org/10.1007/s00704-013-1062-2

Anandhi A, Srinivas V. V., Nanjundiah R, Kumar N (2008) Downscaling Precipitation to River Basin in India for IPCC SRES Scenarios Using Support Vector Machine. Int J Climatol 28:401–420.

https://doi.org/10.1002/joc.1529

Audit IS (2018) Report of the Comptroller and Auditor General of India on Economic Sector, Government of Maharashtra, Report No. 1 of 2018

Bandyopadhyay A, Bhadra A, Raghuwanshi NS, Singh R (2009) Temporal Trends in Estimates of Reference Evapotranspiration over India. J Hydrol Eng 14:508–515. https://doi.org/10.1061/(asce)he.1943-5584.0000006

Chattopadhyay N, Hulme M (1997) Evaporation and potential evapotranspiration in India under conditions of recent and future climate change Evaporation and potential evapotranspiration in India under conditions of recent and future climate change. Agric For Meteorol 87:55–73. https://doi.org/10.1016/S0168-1923(97)00006-3

Chiew FH., Kirono DG., Kent D., et al (2010) Comparison of runoff modeled using rainfall from different downscaling methods for historical and future climates. J Hydrol 387:10–23. https://doi.org/10.1016/j.jhydrol.2010.03.025

Doria R, Madramootoo CA, Mehdi BB (2006) Estimation of future crop water requirements for 2020 and 2050, using CROPWAT. In: 2006 IEEE EIC Climate Change Technology Conference, EICCCC 2006

Duhan D, Pandey A, Gahalaut KPS, Pandey RP (2013) Spatial and temporal variability in maximum, minimum and mean air temperatures at Madhya Pradesh in central India. Comptes Rendus - Geosci 345:3–21. https://doi.org/10.1016/j.crte.2012.10.016

Gade S, Yadav J, Shinde S, et al (2021) Variability in soil moisture using AMSR-E product- A regional case study in the province of Marathwada division, India. Geol Ecol Landscapes. https://doi.org/10.1080/24749508.2021.1943811

Gagnon S, Singh B, Rousselle J, Roy L (2005) An Application of the statistical downscaling model (SDSM) to simulate climatic data for streamflow modelling in Québec. Can Water Resour J 30:297–314. https://doi.org/10.4296/cwrj3004297

Gebremeskel S, Liu YB, DeSmedt F, et al (2004) Analysing the effect of climate changes on streamflow using statistically downscaled GCM scenarios. Int J River Basin Manag 2:271–280. https://doi.org/10.1080/15715124.2004.9635237

Goyal RK (2004) Sensitivity of evapotranspiration to global warming: A case study of arid zone of Rajasthan (India). Agric Water Manag 69:1–11. https://doi.org/10.1016/j.agwat.2004.03.014

Guhathakurta P, Khedikar S, Menon P, et al (2020) CLIMATE RESEARCH AND SERVICES Observed Rainfall Variability and Changes over Maharashtra State

Guo B, Zhang J, Xu T (2018) Comparison of two statistical climate downscaling models: a case study in the Beijing region, China. Int J Water 12:22–38. https://doi.org/10.1504/IJW.2018.090186

Huang J, Zhang J, Zhang Z, et al (2011) Estimation of future precipitation change in the Yangtze River basin by using statistical downscaling method. Stoch Env Res Risk A 25:781–792. https://doi.org/10.1007/s00477-010-0441-9

IPCC (2013) The Physical Science Basis. Contribution of Working Group I to the Fifth Assessment Report of the Intergovernmental Panel on Climate Change. Cambridge University Press, Cambridge, United Kingdom and New York, NY, USA

IPCC (2002) Climate change and biodiversity. Geneva, Switzerland

IPCC (2007) The Physical Science Basis. Contribution of Working Group I to the Fourth Assessment Report of the Intergovernmental Panel on Climate Change. Cambridge University Press, Cambridge, United Kingdom and New York, NY, USA, pp 214–219

Kranz N, Menniken T, Hinkel J (2010) Climate change adaptation strategies in the Mekong and Orange-Senqu basins : What determines the state-of-play? Environ Sci Policy 13:648–659. https://doi.org/10.1016/j.envsci.2010.09.003

Kumar S (2007) Fourth assessment report of the Intergovernmental Panel on Climate Change: Important observations and conclusions. Curr Sci

Kundu S, Khare D, Mondal A (2017) Future changes in rainfall, temperature and reference evapotranspiration in the central India by least square support vector machine. Geosci Front 8:583–596. https://doi.org/10.1016/j.gsf.2016.06.002

Mahmood R, Babel MS (2013) Evaluation of SDSM developed by annual and monthly sub-models for downscaling temperature and precipitation in the Jhelum basin, Pakistan and India. Theor Appl Climatol 113:27–44. https://doi.org/10.1007/s00704-012-0765-0

Manasa HG, Shivapur AV (2016) Implications of Climate Change on Crop Water Requirements in Hukkeri Taluk of Belagavi District, Karnataka, India. Int J Res Eng Technol 05:236–241. https://doi.org/10.15623/ijret.2016.0506044

Micheal AM (2008) Irrigation: Theory and Practices, 2nd edn. Vikas Publishing House Pvt, Ltd., New Delhi

Mohan S, Ramsundram N (2014) Change and its Impact on Irrigation Water Requirements on Temporal Scale. Irrig Drain Sys Eng 3:. https://doi.org/10.4172/2168-9768.1000118

Pandey RP, Dash BB, Mishra SK, Singh R (2008) Study of indices for drought characterization in KBK

districts in Orissa (India). Hydrol Process 22:1895–1907. https://doi.org/10.1002/hyp.6774

Rajabi A, Babakhani Z (2018) The study of potential evapotranspiration in future periods due to climate change in west of Iran. Int J Clim Chang Strateg Manag 10:161–177. https://doi.org/10.1108/IJCCSM-01-2017-0008

Saraf VR, Regulwar DG (2016) Assessment of Climate Change for Precipitation and Temperature Using Statistical Downscaling Methods in Upper Godavari River Basin, India. J Water Resour Prot 08:31–45. https://doi.org/10.4236/jwarp.2016.81004

Suo MQ, Zhang J, Zhou Q, Li YP (2019) Applicability analysis of SDSM technology to climate simulation in Xingtai City, China. IOP Conf Ser Earth Environ Sci 223:. https://doi.org/10.1088/1755-1315/223/1/012053

Tao X e., Chen H, yu Xu C, et al (2015) Analysis and prediction of reference evapotranspiration with climate change in Xiangjiang River Basin, China. Water Sci Eng 8:273–281. https://doi.org/10.1016/j.wse.2015.11.002

TERI (2014) Assessing climate change vulnerability and adaptation strategies for Maharashtra: Maharashtra State Adaptation Action Plan on Climate Change (MSAAPC) New Delhi: The Energy and Resources Institute

Thomas A (2008) Agricultural irrigation demand under present and future climate scenarios in China. Glob Planet Change 60:306–326. https://doi.org/10.1016/j.gloplacha.2007.03.009

Wang F, Chen Y, Li Z, et al (2019) Assessment of the irrigation water requirement and water supply risk in the Tarim River Basin, Northwest China. Sustain 11:. https://doi.org/10.3390/su11184941

Wang W, Xing W, Shao Q, et al (2013) Changes in reference evapotranspiration across the Tibetan Plateau: Observations and future projections based on statistical downscaling. J Geophys Res Atmos 118:4049–4068. https://doi.org/10.1002/jgrd.50393

Wilby R., Dawson C., Barrow E. (2002) SDSM—A Decision Support Tool for the Assessment of Regional Climate Change Impacts. Environ Model Softw 17:147–159. https://doi.org/10.1016/S1364-8152(01)00060-3

Wilby RL, Dawson C. (2007) SDSM 4.2 – A decision support tool for the assessment of regional climate change impacts

Wilby RL, Harris L (2006) A framework for assessing uncertainties in climate change impacts: Low-flow scenarios for the river Thames, UK. Water Resour Res 42:. https://doi.org/10.1029/2005WR004065

Wilby RL, Wigley TML (1997) Downscaling general circulation model output: A review of methods and

limitations. Prog Phys Geogr 21:530–548. https://doi.org/10.1177/030913339702100403

Wilby RL, Wigley TML (2000) Precipitation predictors for downscaling: Observed and general circulation model relationships. Int J Climatol 20:641–661. https://doi.org/10.1002/(SICI)1097-0088(200005)20:6<641::AID-JOC501>3.0.CO;2-1

Xu YP, Pan S, Fu G, Xujie Z (2014) Future potential evapotranspiration changes and contribution analysis in Zhejiang Province, East China. J Geophys Res Atmos 118:2174–2192. https://doi.org/10.1002/2013JD021245.Received

Xu YP, Zhang X, Ran Q, Tian Y (2013) Impact of climate change on hydrology of upper reaches of Qiantang River Basin, East China. J Hydrol 483:51–60. https://doi.org/10.1016/j.jhydrol.2013.01.004

Zeng Z, Wu W, Zhou Y, et al (2019) Changes in reference evapotranspiration over Southwest China during 1960-2018: Attributions and implications for drought. Atmosphere (Basel) 10:. https://doi.org/10.3390/atmos10110705

Zhai P, Zhang Z, Wan H, Pan X (2005) Trends in Total Precipitation and Frequency of Daily Precipitation Extremes over China. J Clim 18:1096–1108. https://doi.org/10.1175/JCLI-3318.1

Zhou T, Wu P, Sun S, et al (2017) Impact of future climate change on regional crop water requirement-A case study of Hetao irrigation district, China. Water (Switzerland) 9:. https://doi.org/10.3390/w9060429

Zotarelli L, Dukes M., Romero C., et al (2010) Step by Step Calculation of the Penman-Monteith Evapotranspiration (FAO-56 Method). Agric Biol Eng